ISBN: 978-3-95450-216-5 doi:10.18429/JACoW-eeFACT2018-WEOAB01

COMMISSIONING STATUS OF SuperKEKB VACUUM SYSTEM

K. Shibata†, Y. Suetsugu, T. Ishibashi, K. Kanazawa, M. Shirai, S. Terui, and H. Hisamatsu
High Energy Accelerator Research Organization (KEK), 305-0817 Tsukuba, Ibaraki, Japan

Abstract

In the upgrade from the KEKB B-factory (KEKB) to the SuperKEKB, approximately 90% and 20% of the beam pipes and vacuum components of the positron ring and the electron ring, respectively, were replaced with new ones. In the Phase-1 commissioning in 2016, vacuum scrubbing and confirmation of the stabilities of new vacuum components at approximately 1 A were carried out, and some problems, such as pressure bursts accompanied with beam losses, were revealed. During the subsequent shutdown, the countermeasures against the problems were taken, and new beam pipes and components, such as beam pipes for the interaction point, and beam collimators were installed. The Phase-2 commissioning, where beam collision tuning was mainly performed, was carried out from March to July 2018. The collimators suppressed the background noise of the particle detector for high-energy physics (Belle II detector) very well, and the frequency of the pressure burst drastically decreased though typical beam currents were lower than those in Phase-1. So far, the vacuum system of the SuperKEKB has been working generally well, and no serious problems have been observed.

INTRODUCTION

The SuperKEKB [1], which is an upgrade of the KEKB, is a high-luminosity electron–positron collider. The main ring (MR) of the SuperKEKB with a circumference of 3016 m is composed of two rings, i.e., the high-energy ring (HER) for 7.0 GeV electrons and the low-energy ring (LER) for 4.0 GeV positrons. Over a period of 10 years, the SuperKEKB project is expected to achieve a 50-fold increase in the integrated luminosity over the original KEKB. The design luminosity is 8.0×10^{35} $cm^{-2}{\cdot}s^{-1}$, which is approximately 40 times the KEKB's record. In the SuperKEKB, the luminosity will be increased by increasing the beam current to 2.6 A (electrons) and 3.6 A (positrons), which are twice as much as in the KEKB, and adopting a novel "nanobeam" collision scheme, which requires a much smaller emittance beam than the KEKB. In order to achieve this challenging goal, many upgrades are required, among which the upgrade of the vacuum system [2-4] is a crucial requirement.

After more than five years of upgradation work on the KEKB, the commissioning of the SuperKEKB commenced in 2016, and two of three commissioning phases have been completed so far. The first commissioning (Phase-1), which was dedicated to accelerator tuning without the Belle II detector [5], was carried out from February to June 2016 [6]. During the subsequent shutdown period, the remained upgradation works including the "roll-in" of the Belle II detector [5] to the collision point were performed. The second commissioning (Phase-2), where beam collision tuning was mainly performed, was carried out from March to July 2018.

† kyo.shibata@kek.jp

VACUUM SYSTEM UPGRADATION

Outline of Upgradation

For the LER, in order to realize small beam emittance, the beam optics was drastically changed compared to that of the KEKB, and a large number of magnets need to be rearranged, replaced, and added. Consequently, approximately 93% of the beam pipes and vacuum components were replaced with new ones. On the other hand, in the HER, the wiggler section was newly made to reduce the emittance, but in the arc sections, no replacement of the magnet was performed. Furthermore, because the beam energy of the HER is reduced from 8.0 GeV to 7.0 GeV, the power of the synchrotron radiation (SR) decreases to the tolerance level of a conventional copper beam pipe, in spite of doubling the beam current. Therefore, approximately 80% of the components in the HER can be reused. Only in the interaction region and the new wiggler section, the beam pipes and components were replaced with new ones. Figure 1 shows the location where the vacuum components were replaced in both rings. The reused components of the HER were left undisturbed in the tunnel during the upgradation work keeping vacuum inside although all vacuum pumps were tuned off. However, these components were sometimes exposed to air temporarily when broken components were replaced with new ones.

The target vacuum pressure in the MR is on the order of 10^{-7} Pa at the designed beam current. In the LER, because of the higher beam currents, the SR power and the photon density are consequently higher, and the resultant heat and gas loads are also larger than those of the KEKB. As a solution to this issue, an effectively distributed pumping scheme using a strip-type NEG (ST707, SAES GETTERS Co. Ltd.) was adopted as the main pump for the arc sections of the LER. The expected effective linear pumping speed is approximately 0.14 $m^3{\cdot}s^{-1}{\cdot}m^{-1}$ for CO just after the NEG activation. In order to achieve the required pressures, a linear pumping speed of approximately 0.1 $m^3{\cdot}s^{-1}{\cdot}m^{-1}$ is required if we assume a photodesorption coefficient of 1×10^{-6} molecules·photon^{-1}, which was obtained at a beam dose of 3×10^3 A·h in the KEKB and will be accrued after approximately 1 year beam operation at the designed beam current in the case of the SuperKEKB. To evacuate non-active gases and to enable more efficient evacuation in relatively high-pressure regimes, noble-type sputter ion pumps with a nominal pumping speed of 0.4 $m^3{\cdot}s^{-1}$ are provided as an

ISBN: 978-3-95450-216-5 doi:10.18429/JACoW-eeFACT2018-WEOAB01

auxiliary pump every 10 m along the ring. The total pressures were measured with approximately 300 cold cathode gauges (CCG, Model C-5, DIAVAC Ltd. Japan) in each ring at pumping ports.

Almost all beam pipes were pre-baked (150 °C, 24 h) [3] in the laboratory before the installation, and no in-situ baking was performed. All beam pipes for the LER were coated with TiN films [7-8] with a thickness of 200 nm to reduce secondary electron yield before the installation as a countermeasure against the electron cloud effect (ECE). To suppress the ECE, additional countermeasures, such as beam pipes with antechambers, a solenoid field, a grooved surface, and an electron clearing electrode, were also adopted in the LER [4].

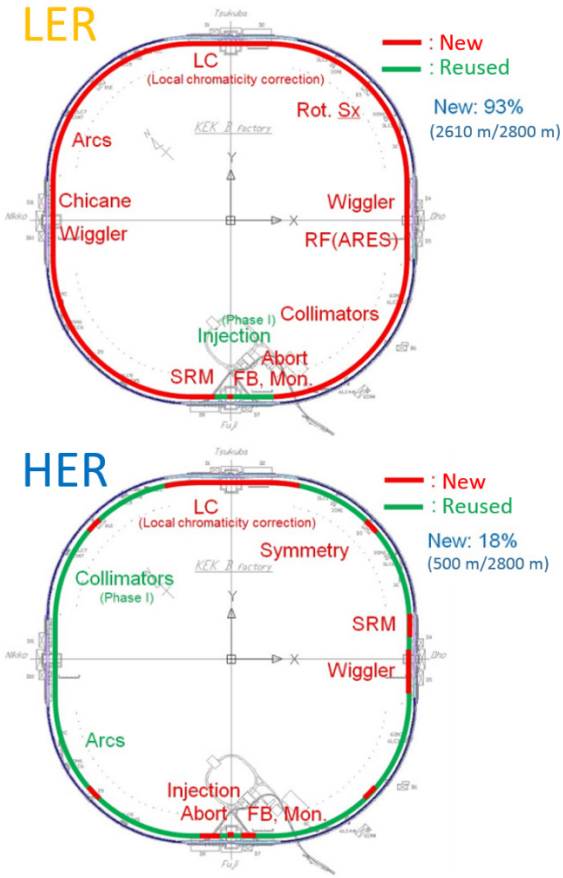

Figure 1: Locations where the vacuum components were replaced in the upgrade from the KEKB to the SuperKEKB.

New Components

Most of the new beam pipes have antechamber structures [3-4, 9], which deal with high power SR due to high beam current, as shown schematically in Fig. 2. SR passes through one or two antechambers at the arc sections or wiggler sections, respectively. At the arc sections, one of the antechambers is used as a pump channel. A screen with many holes with a diameter of 4 mm and a thickness of 5 mm that shields the pump from the beam is installed in the antechamber between the pump and the beam. In the wiggler sections, SR hits both sides of the beam pipe. The beam pipes have no pumping channel. Instead, the pumping ports are located at the bottom of the antechambers in this case. Cooling channels are provided outside the antechambers to absorb heat deposited by SR, beam-induced wall currents, and higher order modes (HOMs). The antechamber plays a key role as a countermeasure against the ECE by minimizing the impact of photoelectrons on the beam [10]. As a countermeasure against the ECE, the beam pipes in the dipole magnets of the LER have grooved surfaces [11] on the upper and lower sides of the beam channel, as shown in Fig. 3. The material of the new beam pipes in the arc sections is Al-alloy, though copper beam pipes are also used at the locations where the SR power is higher, such as the wiggler sections.

Bellows chambers have to be installed between the beam pipes to ease beam–pipe installation and to absorb thermal deformation during the beam operation. More than 1200 bellows chambers are used in one ring. Newly installed bellows chambers have a comb-type RF-shield [12], as shown in Fig. 4, which has a higher thermal strength than a conventional finger-type shield. A comb-type RF-shield was also used for approximately 40 gate valves.

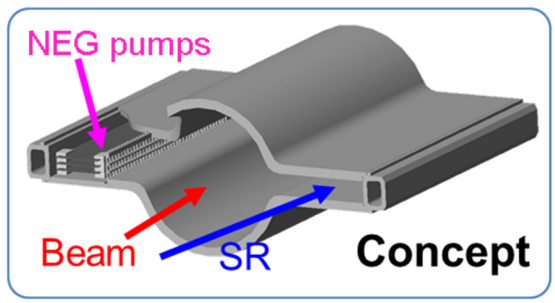

Figure 1: Conceptual drawing of the beam pipe with antechambers for the SuperKEKB.

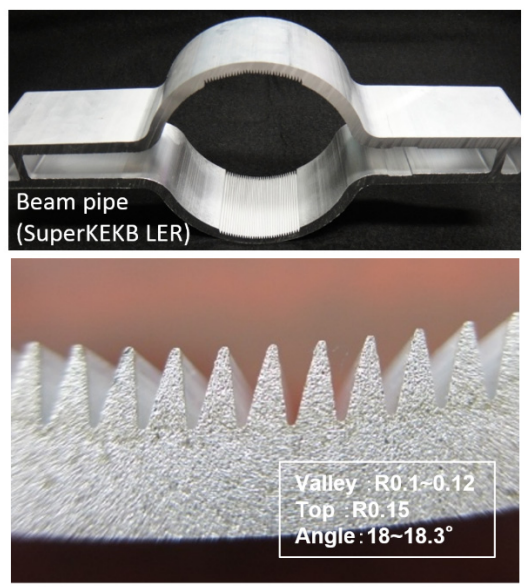

Figure 3: Grooved structure on the top and bottom of the beam channel of the new beam pipe.

ISBN: 978-3-95450-216-5 doi:10.18429/JACoW-eeFACT2018-WEOAB01

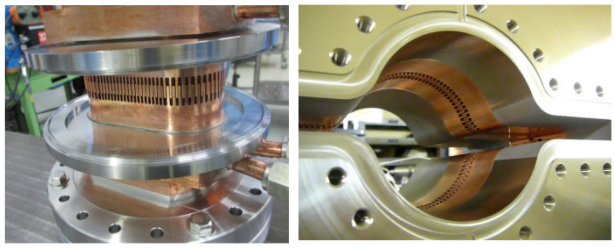

Figure 4: Comb-type RF-shield for new bellows chambers and gate valves for the SuperKEKB.

The beam with a high bunch current (1.4 mA·bunch^{-1}) and a short bunch length (6–7 mm) of the SuperKEKB is likely to excite HOMs. The beam impedance of various vacuum components should be minimized to keep the beam stable and also to avoid excess heating of the components. Gaps or steps at the connection flanges of the beam pipes and the bellows chambers can be significant sources of impedance because the number of flanges is high. As a countermeasure against this issue, step-less Matsumoto–Ohtsuka-type (MO-type) flanges [13], which can provide a vacuum-tight seal at the inner surface while maintaining smooth flow of the wall current across a copper or aluminum-alloy gasket, were adapted to the new components. Figure 5 shows several types of the MO-type flanges adopted in the SuperKEKB. The ante-chamber is also effective in reducing the impedance of SR masks and pumping ports, which are placed in the ante-chambers. The SuperKEKB is the first machine that adopted a comb-type RF-shield and step-less MO-type flanges in a large quantity.

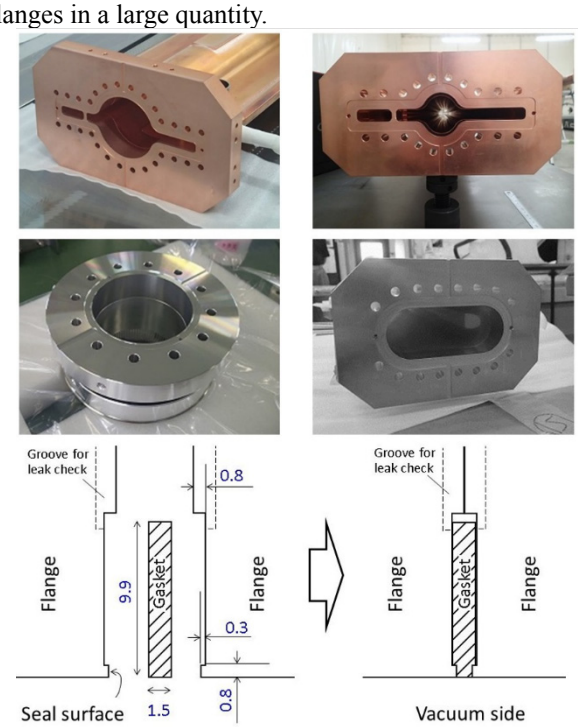

Figure 5: Several types of the step-less MO-type flanges of the SuperKEKB.

New beam collimators [14], which cut off the beam halo and reduce the background noise of the Belle II detector, were installed into the SuperKEKB. These collimators were newly designed based on those used in PEP II at SLAC with the objective of minimizing the impedance. The conceptual structure of the horizontal collimator is shown in Fig. 6. Two new horizontal beam collimators were installed before the Phase-1 commissioning to test during Phase-1. In the HER, 16 KEKB-type beam collimators [15-16] were reused.

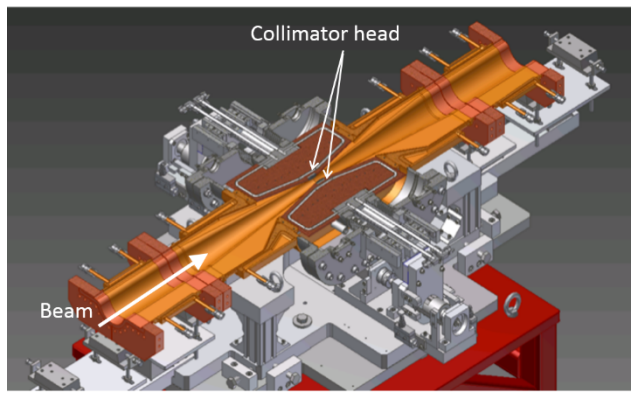

Figure 6: Conceptual structure of new beam collimator (horizontal type).

PHASE-1 COMMISSIONING

Vacuum Scrubbing

The Phase-1 commissioning, which was dedicated to accelerator tuning without the Belle II detector, began in February 2016 and successfully ended in June 2016. Vacuum scrubbing and confirmation of the stabilities of new vacuum components at approximately 1 A were also carried out, and the vacuum system experienced no serious problems during the Phase-I commissioning [17-18]. Figure 7 shows the histories of the average pressure in the whole ring, including that in the straight sections (such as the wiggler sections, beam injection sections, and accelerating cavity sections), average pressure in only the arc sections, and stored beam currents for both rings. The arrows and dates at the tops of Fig. 7 indicate the NEG conditioning times. During Phase-1, the maximum stored beam currents were 1.01 A and 0.87 A and the beam doses were 780 A·h and 660 A·h for the LER and the HER, respectively. For the whole LER, the base pressure (p_{base}) and the average pressure at the maximum beam current (p_{max}) were 5×10^{-8} Pa and 1×10^{-6} Pa, respectively. The p_{max} of the whole ring and that of the arc sections, where most of the beam pipes were newly fabricated, were almost the same. On the other hand, the p_{base} and p_{max} of the whole HER were 3×10^{-8} Pa and 2×10^{-7} Pa, respectively. In the arc sections, the p_{max} was 6×10^{-8} Pa, where most beam pipes were reused from KEKB.

Figure 8 shows the average pressures normalized by a unit beam current, i.e., the pressure rise dp/dI [Pa·mA^{-1}] for the LER and the HER, as functions of the beam doses. In the calculation of dp/dI, the average pressure was used instead of the pressure increase for simplicity. In each graph, the upper axis represents the photon dose D [photons·m^{-1}] in the arc sections, and the right axis indicates

ISBN: 978-3-95450-216-5 doi:10.18429/JACoW-eeFACT2018-WEOAB01

the photon stimulated desorption (PSD) rate η [molecules·photon^{-1}] in the arc section, evaluated by assuming linear pumping speeds of 0.06 m^3·s^{-1}·m^{-1} and 0.03 m^3·s^{-1}·m^{-1} for the LER and the HER, respectively, considering saturation of the NEG pumping speed [2]. For the arc sections in the LER, at the initial stage, η (1×10^{-3} molecules·photon^{-1}) is several times lower than its value in the KEKB (4×10^{-3} molecules·photon^{-1}), where circular copper beam pipes without any coating were used [19]. However, at the final stage ($D = 4 \times 10^{24}$ photons·m^{-1}), η (7×10^{-6} molecules·photon^{-1}) has almost the same value as in the KEKB at the same photon dose. The slope η gradually increases with increasing D. Note that η slightly increased when $D > 6 \times 10^{23}$ photons·m^{-1}. The main cause for this increase was a nonlinear increase in the pressure with increasing the beam current due to the gas desorption from electron multipacting in the beam pipe [17-18]. Therefore, the η values in this region do not reflect the real PSD rate. In the HER, on the other hand, the η is lower and shows a steeper decrease in the early stage compared to that in the LER. The η decreases less rapidly at $D > 1 \times 10^{24}$ photons·m^{-1}, but this change occurs because the effect of the base pressure is not negligible in the dp/dI calculations. That η in the HER is lower than that in the HER of the KEKB from the beginning [19]. The η at the final stage (1×10^{-7} molecules·photon^{-1}) is much lower than that in the case of the KEKB (2×10^{-6} molecules·photon^{-1}) at the same D, and its value is almost the same as that in the final stage of the KEKB [19]. Since most of the beam pipes in the arc sections of the HER were reused from the KEKB, their surfaces "remember" the conditions in the KEKB after sufficient vacuum scrubbing (memory effect), even though they were sometimes exposed to air for the vacuum work.

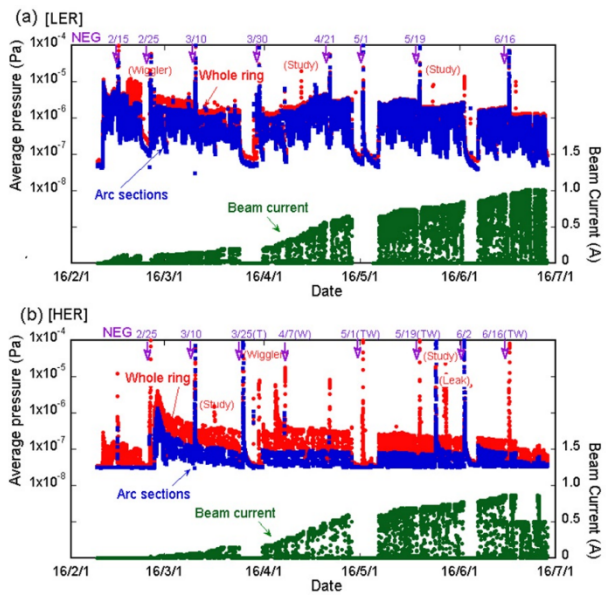

Figure 7: Histories of the average pressures in the whole ring (red), those in the arc sections (blue), and the stored beam currents (green) for (a) the LER and (b) the HER, respectively, during the Phase-1 commissioning.

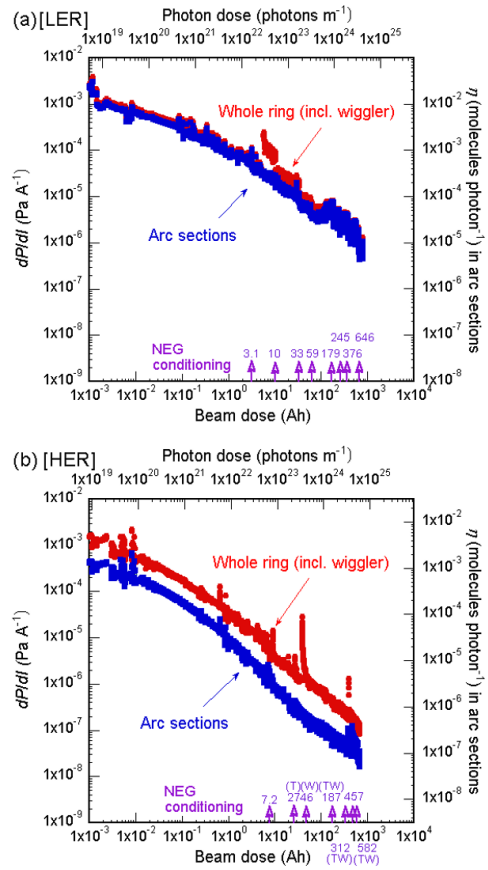

Figure 8: Average pressures normalized by a unit beam current dp/dI for (a) the LER and (b) the HER, respectively, as functions of the beam dose during Phase-1. The PSD rate η in the arc sections as a function of the photon dose is also shown in each graph.

Status of the New Vacuum Components

The SuperKEKB is the first machine to adopt step-less MO-flanges and comb-type RF-shields on a large scale. During the Phase-1 commissioning no overheating, discharging, or abnormal pressure increases were observed in these components. The average temperature increase of these components is less than 4 °C at 1 A. The temperature increases in the bellows chambers located near the beam collimator, where extra HOMs are easily excited, are less than 2 °C, though overheating of the bellows chambers with a conventional finger-type RF-shield was frequently observed in the KEKB.

As for the beam collimators, their operability, heating, and collimator head position accuracy were checked using high beam currents. The effectiveness of the background noise reduction was also confirmed by a preliminary detector installed near the collision point.

Major Problems

One of the major concerns during the Phase-1 commissioning was the localized pressure burst phenomenon accompanied with beam loss in the LER [20-21]. The beam loss monitors triggered beam aborts, and sometimes pressure bursts became obstacles during the beam com-

ISBN: 978-3-95450-216-5 doi:10.18429/JACoW-eeFACT2018-WEOAB01

missioning. Most of the pressure bursts occurred near or inside Al-alloy beam pipes with grooved surfaces in dipole magnets. The beam current, at which the bursts occurred, increased gradually with the maximum stored beam current (I_{max}). Figure 9 shows the numbers of bursts occurring per 50 h of the operation time (red bars), beam currents when the pressure bursts occurred (blue circles), and I_{max} (black lines) versus the duration of operation with a beam current greater than 50 mA during Phase-1. The most probable cause is collisions between circulating beams and dusts (small particles) in the beam pipes. The longitudinal grooves in the beam pipes in the dipole magnets, which counteract the ECE, are likely to trap dusts during the manufacturing process. Indeed, the pressure bursts and simultaneous beam loss at a beam current of approximately 0.8 A were reproduced by a test using a knocker attached to several beam pipes in the dipole magnets, which impacts the beam pipe to drop dust particles from their ceilings.

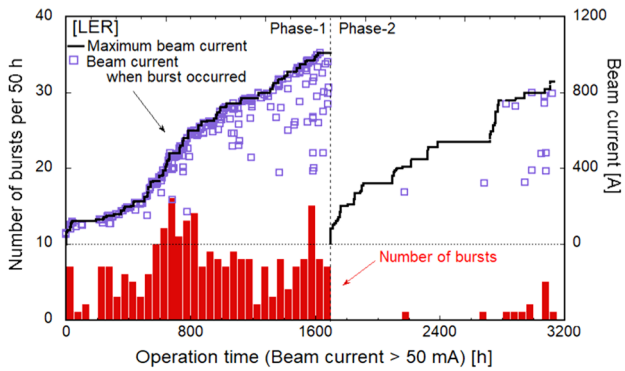

Figure 9: Number of bursts occurring per 50 h of the operation time (red bars), beam currents (blue squares), and maximum stored beam current (black lines) when pressure bursts occurred in the LER during Phase-1 (left) and Phase-2 (right).

Several beam pipes and connection flanges in the LER wiggler sections heated up. It was found that the temperature of them was sensitive to the vertical beam orbit upstream of the beam pipes, and also to the vertical position of the beam pipes themselves. From these results, it was concluded that the heating was caused by SR emitted from the wiggler magnets' upstream of the beam pipes in question. The beam pipes and the connection flanges in the wiggler section have antechambers with a height of 14 mm, which SR can pass through. However, vertically steered SR or SR spreading in the vertical direction emitted from a distance cannot be accommodated completely in the antechambers and irradiates the upper and lower surfaces of the antechambers. Since the SR masks, which are located only at the side of the antechambers, can not prevent the connection flanges from being irradiated by such SR, the connection flanges were overheated, and an air leak due to excess heating was observed through a metal seal of the flanges in the worst case.

In addition, a nonlinear pressure rise due to the ECE was observed. This will not be described here as it will be discussed in detail in other paper [17-18, 21].

WORK FOR PHASE-2

Installation of New Components

The most important work in the MR during the shutdown period before the Phase-2 commissioning was to install new beam pipes and components for the Belle II detector and the superconducting final-focusing magnets (QCS magnets) around the collision point.

Six additional beam collimators were installed to suppress the background noise of the Belle II detector, following successful results of the two models used in the Phase-1 commissioning. Including the KEKB-type beam collimators reused in the HER, 5 and 19 beam collimators were prepared for the LER and the HER, respectively, for the Phase-2 commissioning.

The beam pipes at the LER injection region were changed to adapt a low emittance beam injected through the new positron damping ring [23-24].

Countermeasures Against Major Problems

During this shutdown period, we gathered dusts from the beam pipe where bursts were frequently observed by a special tool to clean up the inside of the beam pipes. Actually, we found large-size Al and Al_2O_3 particles in one of the beam pipes where pressure bursts were frequently observed in Phase-1. Furthermore, we knocked most of the beam pipes, in which pressure bursts were frequently observed, and dropped dust particles from their ceilings prior to starting the Phase-2 commissioning.

As for overheating of the connection flanges and air leak in the wiggler sections, new bellows chambers having SR masks at the top and bottom of the antechambers were fabricated for protecting the connection flanges from vertically steered or spreading SR. Two bellows chambers with masks were installed between the beam pipes in the wiggler section. Furthermore, the beam pipes were realigned in the vertical direction with respect to the nearby quadrupole magnets. The beam orbit in the wiggler section was kept as flat as possible during the beam operation in the Phase-2 commissioning. Additionally, the flow rate of cooling water for the overheated beam pipes was increased as much as possible.

PHASE-2 COMMISSIONING

Vacuum Scrubbing

The Phase-2 commissioning began in March 2018 and ended in July 2018. The vacuum system worked generally well and experienced no serious problems again during the Phase-2 commissioning. Figure 10 shows the histories of the average pressure in the whole ring, including that in the straight sections, average pressure in only the arc sections, and stored beam current for both rings. Since the major task of the Phase-2 commissioning was beam collision tuning to verify the novel "nanobeam" collision scheme, typical stored beam currents during Phase-2 were lower than those during Phase-1. However, at the latter in the Phase-2 commissioning, the stored beam currents were increased gradually to confirm the stabilities of

ISBN: 978-3-95450-216-5 doi:10.18429/JACoW-eeFACT2018-WEOAB01

newly installed vacuum components, but the operation time with high currents was not so long. During Phase-2, the maximum stored beam currents were 0.86 A and 0.80 A in the LER and the HER, respectively, and the beam doses were 340 A·h for both rings. For the whole LER, the p_{base} and p_{max} were 5×10^{-8} Pa and 3×10^{-7} Pa, respectively. The p_{max} of the arc sections was 1×10^{-7} Pa. On the other hand, the p_{base} and p_{max} of the whole HER were 3×10^{-8} Pa and 7×10^{-8} Pa, respectively. In the arc sections, the p_{max} was 4×10^{-8} Pa. The lifetime was determined mainly by the Touschek effect in both rings.

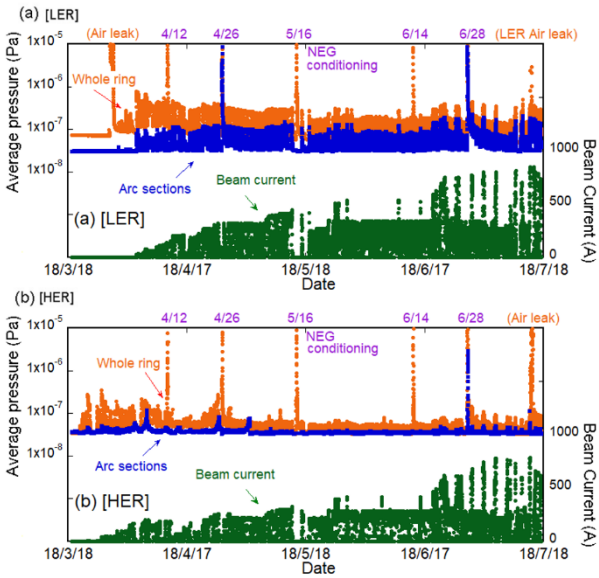

Figure 10: Histories of the average pressures in the whole ring (red), those in the arc sections (blue), and the stored beam currents (green) for (a) the LER and (b) the HER, respectively, during the Phase-2 commissioning.

Figure 11 shows dp/dI for the LER and the HER as a function of the beam dose during the Phase-2 commissioning. At the initial stage, the dp/dI values were high, because vacuum works, such as installation of new beam pipes around the collision point, were carried out during the shutdown period. However, the dp/dI decreased steadily with increasing the beam dose. Figure 12 shows the dp/dI for the whole rings and η in the arc sections for the LER and the HER during the Phase-1 and Phase-2 commissioning. For the LER, it was found that the η values at the last stage of the Phase-2 commissioning are less than those of the Phase-1 commissioning. The decrease in η during Phase-2 is very clear, because a nonlinear pressure increase due to the ECE was suppressed in Phase-2 by the installation of permanent magnets [24]. For the HER, on the other hand, the decrease in η during Phase-2 is not clear, because the p_{max} is too low to calculate the dp/dI accurately.

So far, the total beam dose has been 1113 A·h and 1002 A·h for the LER and the HER, respectively. At the end of the Phase-2 commissioning, the dp/dI values for the whole ring were approximately 3×10^{-7} Pa·A^{-1} and 7×10^{-8} Pa·A^{-1} for the LER and the HER, respectively. In the arc sections, the total photon doses reached 5.9×10^{24} photons·m^{-1} and 9.3×10^{24} photons·m^{-1}, for the LER and the HER, respectively at the end of Phase-2, and η decreased to 1×10^{-6} molecules·photon^{-1} and 7×10^{-8} molecules·photon^{-1} for the LER and the HER, respectively.

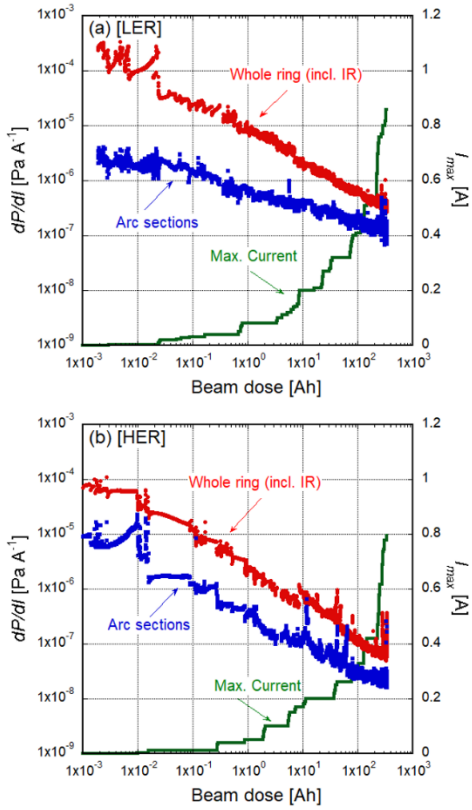

Figure 11: Average pressures normalized by a unit beam current dp/dI and the maximum beam current for (a) the LER and (b) the HER, respectively, as functions of the beam dose during Phase-2.

Status of the New Vacuum Components

The newly installed vacuum components worked well, and vacuum scrubbing of those components processed smoothly as described above.

The tuning of beam collimators watching the detector background and the beam injection rate was carried out. The beam collimators suppressed the background noise of the Belle II detector well and prevented the QCS magnets from quenching caused by the penetration of the particles deviated from their ideal orbit.

Effect of Countermeasures Against Problems in Phase-1

The number of bursts per 50 h of the operation time, beam currents when bursts occurred, and maximum beam currents as functions of the total beam operation time during the Phase-2 commissioning are shown in Fig. 9. The frequency of pressure bursts was greatly reduced in Phase-2. However, the frequency of pressure bursts reduced not only at the locations where the beam pipes were knocked, but also at other locations. Therefore, it

ISBN: 978-3-95450-216-5 doi:10.18429/JACoW-eeFACT2018-WEOAB01

cannot be determined yet whether it is effective to knock the beam pipes or not. During Phase-2, the operation time with low currents for the collision tuning was long, and the operation time with high beam currents was much shorter than that during Phase-1. This may be one of the causes for the reduction in the frequency of pressure bursts.

Overheating of the beam pipes and connection flanges in the wiggler sections were still observed, though the temperature rise became smaller than that in Phase-1. However, there was no air leak at the connection flanges during Phase-2. This indicates that countermeasures, such as the new bellows chamber with SR masks at the top and bottom of the antechambers, functioned well. This overheating was not a particularly serious problem in Phase-2, but in Phase-3, it will be necessary to enhance the cooling of the beam pipe, for example by attaching a cooling block.

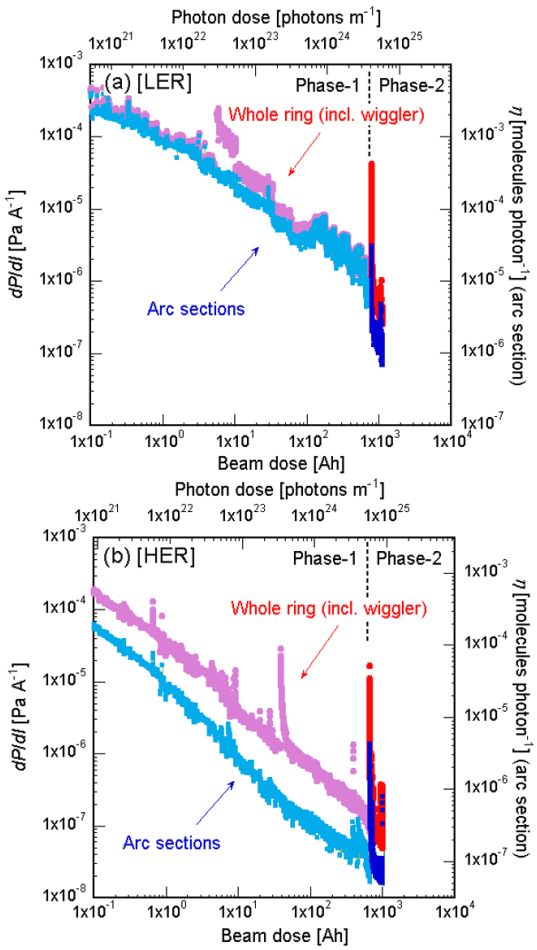

Figure 12: Average pressures normalized by a unit beam current dp/dI for (a) the LER and (b) the HER, respectively, as functions of the beam dose during Phase-1 and Phase-2. The PSD rate η in the arc sections as a function of the photon dose is also shown in each graph.

Major Problems

During the beam operation, the beam of the LER suddenly became unstable, and the intense beam hit the newly installed collimator head directly. As a result, a groove and protrusions were formed on the surface of the collimator head. The damaged collimator head is shown in Fig. 13. This collimator has been very effective in reducing the background so far. However, when this damaged collimator head was brought close to the beam, the background noise did not decrease, but increased. As a temporary countermeasure against this problem, the collimator chamber was slightly moved to make the undamaged surface of the collimator head available, so that the collimator functioned well again. The damaged heads will be replaced with new ones during the subsequent shutdown period.

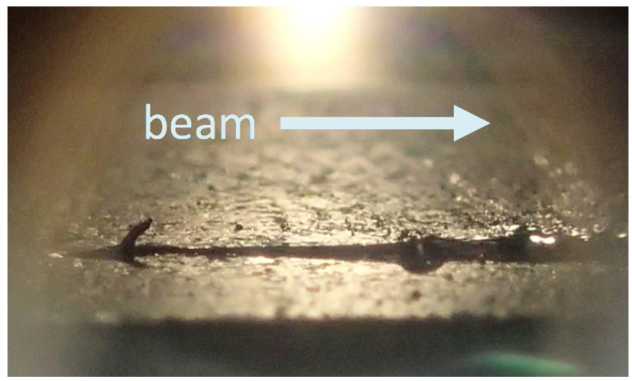

Figure 13: Groove and protrusions formed on the surface of the collimator head.

Two stainless steel beam pipes (inner copper plating), which had been installed at 15–20 m downstream of the collision point in the HER before the Phase-1 commissioning, exhibited overheating and air leaks. The cause for the overheating was SR emitted from the QCS magnet. This SR irradiation was not taken into consideration when designing the beam pipes, and there were no SR masks to prevent these stainless steel beam pipes from being directly irradiated by SR emitted from the QCS magnet. Air leaks occurred between the stainless steel MO-type flange and the copper MO-type flange, and the cause for the air leaks is considered to be the heat cycle. As a countermeasure against this problem, beam pipes and bellows chambers with SR masks will be installed at the upstream. We are also studying the fabrication of stainless steel beam pipes with the copper MO-type flanges.

SUMMARY

Through the Phase-1 and Phase-2 commissioning of the SuperKEKB, in which the total beam doses exceeded 1000 A·h, the vacuum system worked generally well. The pressures of both rings decreased according to our expectations, though the pressure of the LER was still higher than that of the HER. The newly adopted components, such as MO-type flanges, comb-type RF-shielding, beam pipes with antechambers, and new collimator, have functioned well so far.

During the shutdown period before the Phase-3 commissioning, the beam pipe for the interaction point is once removed for the upgradation work of the Belle II detector

ISBN: 978-3-95450-216-5 doi:10.18429/JACoW-eeFACT2018-WEOAB01

and reinstalled into the SuperKEKB again with the completed Belle II detector. Five new collimators are installed mainly into the LER, and damaged mask heads are replaced with new ones.

The Phase-3 commissioning will commence in March 2019. It is necessary to continue to monitor carefully whether new problems associated with an increase in the beam current in the vacuum system occur.

ACKNOWLEDGEMENTS

The authors would like to thank colleagues in the SuperKEKB team.

REFERENCES

[1] SuperKEKB, http://www-superkekb.kek.jp

[2] Y. Suetsugu *et al.*, "Design and construction of the SuperKEKB vacuum system", *J. Vac. Sci. Technol. A*, vol. 30(3), p. 031602, 2012, doi:10.1116/1.3696683.

[3] Y. Suetsugu *et al.*, "Construction status of the SuperKEKB vacuum system", *Vacuum*, vol. 121, pp. 238-244, 2015.

[4] Y. Suetsugu *et al.*, "Results and problems in the construction phase of the SuperKEKB vacuum system", *J. Vac. Sci. Technol. A*, vol. 34(2), p. 021605, 2016, doi:10.1116/1.4942455.

[5] Belle II, https://www.belle2.org

[6] Y. Ohnishi *et al.*, "COMMISSIONING OF THE PHASE-1 SuperKEKB B-FACTORY AND UPDATE ON THE OVERALL STATUS", in *Proc. NAPAC2016,* Chicago, IL, USA, Oct. 2016, pp. 32-36.

[7] K. Shibata, H. Hisamatsu, K. Kanazawa, Y. Suetsugu, M. Shirai, "DEVELOPMENT OF TiN COATING SYSTEM FOR BEAM DUCTS OF KEK B-FACTORY", in *Proc. EPAC'08, Genoa*, Italy, June 2008, pp. 1700-1702.

[8] Y. Suetsugu, K. Kanazawa, K. Shibata, H. Hisamatsu, "Recent studies on photoelectron and secondary electron yields of TiN and NEG coating using the KEKB positron ring", *Nucl. Instrum. Methods Phys. Res. A*, vol. 578(3), pp. 470-479, 2007, doi:10.1016/j.nima.2007.06.015.

[9] Y. Suetsugu, K. Shibata, H. Hisamatsu, M. Shirai, K. Kanazawa, "Development of copper beam ducts with antechambers for advanced high-current particle storage rings", *Vacuum*, vol. 84(5), pp. 694-698, 2010.

[10] J. A. Crittenden, T. Ishibashi, and Y. Suetsugu, "SYNCHROTRON RADIATION ANALYSIS OF THE SUPERKEKB POSITRON STORAGE RING", in *Proc. IPAC'15,* Richmond, VA, USA, May 2015, pp. 2222-2225, doi:10.18429/JACoW-IPAC2015-TUPTY080.

[11] Y. Suetsugu, H. Fukuma, M. Pivi, and L. Wang, "Continuing study on electron-cloud clearing techniques in high-intensity positron ring: Mitigation by using groove surface in vertical magnetic field", *Nucl. Instrum. Methods Phys. Res. A*, vol. 604(3), pp. 449-456, 2009, doi:10.1016/j.nima.2009.03.011.

[12] Y. Suetsugu *et al.*, "Development of bellows and gate valves with a comb-type rf shield for high-current accelerators: Four-year beam test at KEK B-Factory", *Rev. Sci. Instrm.*, vol. 78(4), p. 043302, 2007, doi:10.1063/1.2723747.

[13] Y. Suetsugu, M. Shirai, and M. Ohtsuka, "Application of a Matsumoto-Ohtsuka-type vacuum flange to beam ducts for future accelerators", *J. Vac. Sci. Technol. A*, vol. 23(6), pp. 1721-1727, 2005, doi:10.1116/1.2101808.

[14] T. Ishibashi, S. Terui, and Y. Suetsugu, "LOW IMPEDANCE MOVABLE COLLIMATORS FOR SUPERKEKB" in *Proc. IPAC'17*, Copenhagen, Denmark, May 2017, pp. 2929-2932.

[15] Y. Suetsugu, T. Kageyama, K. Shibata, and T. Sanami, "Latest movable mask system for KEKB", *Nucl. Instrum. Methods Phys. Res. A*, vol. 513(3), pp. 465-472, 2003, doi:10.1016/j.nima.2003.06.003.

[16] Y. Suetsugu, K. Shibata, T. Sanami, T. Kageyama, and Y. Takeuchi, "Development of movable mask system to cope with high beam current", *Rev. Sci. Instrm.*, vol. 74(7), pp. 3297-3304, 2003, doi:10.1063/1.1583860.

[17] Y. Suetsugu *et al.*, "Achievements and problems in the first commissioning of superKEKB vacuum system", *J. Vac. Sci. Technol. A*, vol. 35(3), p. 03E103, 2017, doi:10.1116/1.4977764.

[18] Y. Suetsugu *et al.*, "First commissioning of the SuperKEKB vacuum system", *Phys. Rev. ST Accel. Beams,* vol. 19(12), p. 121001, 2016, doi:10.1103/PhysRevAccelBeams.19.121001.

[19] K. Kanazawa *et al.*, "Experiences at the KEK B-factory vacuum system", *Prog. Theor. Exp. Phys.*, vol. 2013(3), p. 03A005, 2013, doi: 10.1093/ptep/pts068.

[20] S. Terui *et al.*, "OBSERVATION OF PRESSURE BURSTS IN THE SUPERKEKB POSITRON RING", in *Proc. IPAC'18*, Vancouver, BC, Canada, April 2018, pp. 2830-2832, doi:10.18429/JACoW-IPAC2018-WEPML058.

[21] Y. Suetsugu *et al.*, "STATUS OF THE SuperKEKB VACUUM SYSTEM IN THE PHASE-2 COMMISSIONING", in *Proc. IPAC'18*, Vancouver, BC, Canada, April 2018, pp. 2833-2835, doi:10.18429/JACoW-IPAC2018-WEPML059.

[22] Y. Suetsugu *et al.*, "Study to Mitigate Electron Cloud Effect in SuperKEKB", presented at *eeFACT2018*, Hong Kong, China, September 2018, paper TUYAA04, this conference.

[23] M. Kikuchi *et al.*, "DESIGN OF POSITRON DAMPING RING FOR SUPER-KEKB", in *Proc. IPAC'10*, Kyoto, Japan, May 2016, pp. 1641-1643.

[24] K. Shibata *et al.*, "Vacuum system of positron damping ring for SuperKEKB", *J. Vac. Sci. Technol. A*, vol. 35(3), p. 03E106, 2017, doi:10.1116/1.4979009.